

PUSHING THE PRECISION LIMIT OF ^{14}C AMS

Peter Steier¹ • Franz Dellinger • Walter Kutschera • Alfred Priller • Werner Rom² •
Eva Maria Wild

Vienna Environmental Research Accelerator (VERA), Institut für Isotopenforschung und Kernphysik, Universität Wien,
Währinger Strasse 17, A-1090 Wien, Austria.

ABSTRACT. High precision for radiocarbon cannot be reached without profound insight into the various sources of uncertainty which only can be obtained from systematic investigations. In this paper, we present a whole series of investigations where in some cases $^{16}\text{O}:^{17}\text{O}:^{18}\text{O}$ served as a substitute for $^{12}\text{C}:^{13}\text{C}:^{14}\text{C}$. This circumvents the disadvantages of event counting, providing more precise results in a much shorter time. As expected, not a single effect but a combination of many effects of similar importance were found to be limiting the precision.

We will discuss the influence of machine tuning and stability, isotope fractionation, beam current, space charge effects, sputter target geometry, and cratering. Refined measurement and data evaluation procedures allow one to overcome several of these limitations. Systematic measurements on FIRI-D wood show that a measurement precision of ± 20 ^{14}C yr (1σ) can be achieved for single-sputter targets.

INTRODUCTION

When accelerator mass spectrometry (AMS) for radiocarbon measurements was introduced some 25 yr ago, it was generally believed that it would not be able to reach the precision of beta counting. This was based on the notion that AMS facilities are much more complex and, thus, possess more sources of uncertainty. If counting statistics are improved by extended measurement duration, these systematic errors become significant. Thus, a precise analysis is a prerequisite for improvement.

The archaeologist usually asks for the *accuracy* of data, i.e. the maximum deviation from the “true” sample age. However, we can determine only the *precision* (i.e. the reproducibility of the result) if we would do the same measurement over and over. If only a part of the measurement is repeated (e.g. the AMS measurement but not the sample preparation), the uncertainty is underestimated. In this paper, we focus on samples containing several mg of carbon, where the sample size imposes no limit on counting statistics for AMS.

In a rough classification, uncertainty can be attributed to counting statistics, fractionation, contamination, and limited instrumental precision (e.g. of Faraday cups). Fractionation and contamination take place both in nature and in the laboratory. Carbon contamination already present when the sample arrives in the laboratory has to be carefully removed, because a suitable correction is usually not possible. Contamination in the laboratory is traced by suitable “blank” materials which undergo the same treatment as the samples. Laboratory contamination is more critical for AMS than for decay counting, since the AMS samples are significantly smaller.

In AMS, the ^{14}C content is always measured relative to ^{12}C and/or ^{13}C . These isotopes serve as an intrinsic tracer for the yield of the various processes. Therefore, knowledge of the yield is only of importance for the measurement precision if it differs for the various isotopes. Such fractionation can occur in every step where the yield is less than 100%. Many physical and chemical fractionation processes (both in nature and laboratory) show a simple dependence on the isotope mass, i.e. the

¹Corresponding author. Email: peter.steier@univie.ac.at.

²Present address: Institut für Nanostrukturierte Materialien und Photonik, Joanneum Research,
Franz-Pichler-Strasse 30, A-8160 Weiz, Austria.

fractionation of $^{14}\text{C}/^{12}\text{C}$ is twice the fractionation of $^{13}\text{C}/^{12}\text{C}$. This is called *mass dependent fractionation* by Thiemens (1999) and corresponds to “ $b = 2$ ” in Wigley and Muller (1981). In this paper, we will call it *strictly mass dependent fractionation*. The measured $^{14}\text{C}/^{12}\text{C}$ ratio can be corrected by normalizing the measured $^{13}\text{C}/^{12}\text{C}$ ratio to the nominal value of $\delta^{13}\text{C} = -25\text{‰}$ (Stuiver and Polach 1977). Precise ^{14}C dating relies on the assumption that all natural fractionation before the sample arrives in the laboratory is strictly mass dependent. Whereas AMS allows measuring $^{13}\text{C}/^{12}\text{C}$ in combination with $^{14}\text{C}/^{12}\text{C}$, decay counting requires a separate determination.

Laboratory fractionation effects are large in AMS machines. The main factors are the negative ion yield in the ion source (Nadeau et al. 1987), the stripping efficiency (Finkel and Suter 1993), and the ion-optical transmission through the whole machine. The raw $^{13}\text{C}^{3+}/^{12}\text{C}^{3+}$ and $^{14}\text{C}^{3+}/^{12}\text{C}^{3+}$ ratios measured at VERA deviate by several percent from the “true” isotopic ratios of the sample (see Table 1). This fractionation generally is not strictly mass dependent. It is handled by normalizing to a standard material which is measured together with the unknown samples.

Table 1 Unnormalized isotopic ratios for IAEA C-3 Cellulose. The nominal isotopic signature is $\delta^{13}\text{C} = -24.91 \pm 0.49\text{‰}$ and a ^{14}C content of 129.41 ± 0.06 pMC (percent Modern Carbon). For the $^{13}\text{C}^{3+}$, $^{12}\text{C}^{3+}$, and $^{14}\text{C}^{3+}$ values observed at VERA, we estimate an uncertainty of $<2\%$ from the reproducibility of the data and by comparing the reading of different Faraday cups of the same beam.

	Expected value	Observed at VERA at 2.7 MV	
		Ar stripper gas	O ₂ stripper gas
$^{12}\text{C}^{3+}$ stripping yield	Ar: $\sim 53.8\%$ ^a , O ₂ : $\sim 49.8\%$ ^a	$^{12}\text{C}^{3+}/^{12}\text{C}^{-} = 51.5\%$	$^{12}\text{C}^{3+}/^{12}\text{C}^{-} = 49.5\%$
$^{13}\text{C}/^{12}\text{C}$	1.0957×10^{-2}	$^{13}\text{C}^{3+}/^{12}\text{C}^{3+} = 1.07 \times 10^{-2}$	$^{13}\text{C}^{3+}/^{12}\text{C}^{3+} = 1.01 \times 10^{-2}$
$^{14}\text{C}/^{12}\text{C}$ ^b	1.529×10^{-12}	$^{14}\text{C}^{3+}/^{12}\text{C}^{3+} = 1.38 \times 10^{-12}$	$^{14}\text{C}^{3+}/^{12}\text{C}^{3+} = 1.27 \times 10^{-12}$

^aFinkel and Suter 1993.

^bin 2003.

If the contamination and the sample mass are constant, blank correction can be established by subtracting the measured $(^{14}\text{C}^{3+}/^{12}\text{C}^{3+})_{\text{blank}}$ of a nominally “dead” carbon sample from the measured $^{14}\text{C}^{3+}/^{12}\text{C}^{3+}$ of the unknown sample and the standard material:

$$(^{14}\text{C}^{3+}/^{12}\text{C}^{3+})_{\text{sample, blank corr}} = (^{14}\text{C}^{3+}/^{12}\text{C}^{3+})_{\text{sample}} - (^{14}\text{C}^{3+}/^{12}\text{C}^{3+})_{\text{blank}} \quad (1a),$$

$$(^{14}\text{C}^{3+}/^{12}\text{C}^{3+})_{\text{sample, blank corr}} = (^{14}\text{C}^{3+}/^{12}\text{C}^{3+})_{\text{standard}} - (^{14}\text{C}^{3+}/^{12}\text{C}^{3+})_{\text{blank}} \quad (1b).$$

$^{12}\text{C}^{3+}$, $^{13}\text{C}^{3+}$, and $^{14}\text{C}^{3+}$ denote the particle rates measured in the AMS analyzer. Strictly mass dependent fractionation is cancelled out by calculating

$$F_{12,13,14,\text{sample}} = (^{14}\text{C}^{3+}/^{12}\text{C}^{3+})_{\text{sample, blank corr}} \div (^{13}\text{C}^{3+}/^{12}\text{C}^{3+})_{\text{standard}}^2 \quad (2a),$$

$$F_{12,13,14,\text{standard}} = (^{14}\text{C}^{3+}/^{12}\text{C}^{3+})_{\text{standard, blank corr}} \div (^{13}\text{C}^{3+}/^{12}\text{C}^{3+})_{\text{sample}}^2 \quad (2b).$$

The following equation:

$$\text{pMC}_{\text{sample}} = \frac{F_{12,13,14,\text{sample}}}{F_{12,13,14,\text{standard}}} \times \text{pMC}_{\text{standard, nominal}} \quad (3),$$

performs the normalization to a reference standard with the nominal value $\text{pMC}_{\text{standard,nominal}}$.

These formulas are equivalent to the method described by Stuiver and Polach (1977). Relative measurements increase the precision by canceling out systematic errors. This basic principle is explicitly visible in equations (1), (2), and (3). It also reveals that most aspects of precision can be studied by investigating the reproducibility of the values $F_{12,13,14}$ obtained for samples prepared from the same material. For these investigations, no standard material is needed. The relative precision of $\text{pMC}_{\text{sample}}$ in a measurement including a standard will be the quadratic sum of the reproducibilities obtained for $F_{12,13,14,\text{sample}}$ and $F_{12,13,14,\text{standard}}$.

Fractionation only introduces uncertainty if it is not strictly mass dependent and if it is different for the standard and the unknown sample. A good correction can be expected for the fractionation in the stripping process since it is identical for all sputter targets. Slight variations in the chemical composition of the sputter targets induce fractionation differences in the ion source. However, this fractionation originates mainly in the different initial velocity of the sputtered $^{12}\text{C}^-$, $^{13}\text{C}^-$, and $^{14}\text{C}^-$ (Nadeau et al. 1987), so we expect this to be strictly mass dependent.

Finally, the use of the ^{14}C calibration curve is a normalization to independently dated samples, i.e. to the wood, coral, and varve samples incorporated in INTCAL98 (Stuiver et al. 1998). This applies both for AMS and decay counting and accounts for the varying ^{14}C content of the atmosphere in the past. We do not discuss the uncertainty introduced by the calibration process in this paper.

All measurements reported in this paper were performed at VERA. The standard operation of VERA for ^{14}C measurements was described in Priller et al. (1997) and has been basically maintained until today. Important improvements towards higher precision are described in the following.

Ion Optical Losses

Fractionation caused by ion optical beam losses will happen at every aperture where the transmission is less than 100% and where the beam profiles of ^{12}C , ^{13}C , and ^{14}C are not exactly the same. Geometrical differences of the sputter targets will lead to different beam profiles and, therefore, to different fractionation of the standard and unknown sample.

Two strategies can reduce the resulting systematic uncertainties: first, one can make the sputter target geometry as similar as possible; and second, one can try to eliminate the beam losses.

A source of variation in the sample geometry specific to our ion source (40 samples MC-SNICS; Ferry 1993) is the eccentricity of the sample wheel. As discussed in Puchegger et al. (2000), this can be partially compensated with the first beam steerers after the ion source. The reproducibility of the measured isotopic ratios was especially sensitive to the eccentricity if the whole sample wheel had a displacement bias. Therefore, a mechanism was implemented which allows to move the wheel horizontally and vertically relative to the Cs beam while the $^{12}\text{C}^-$ output of the ion source is monitored. This alignment is performed for every newly mounted wheel and every machine tuning.

Additional geometrical differences of the sputter targets are caused by sputter cratering. To reach the precision goal of less than 40 yr for all targets in the minimum total measurement time in routine ^{14}C measurements, older samples are measured longer than younger samples, resulting in deeper sputter craters. In a systematic measurement (see Figure 1), we investigated this effect up to about 5 hr of sputtering, which is about 3 times longer than the maximum sputter time in a routine measurement. Although no significant trend is visible in this experiment, deviations were observed for targets which were sputtered for extremely long periods (several hours) during machine warm-up and tun-

ing. Therefore, for high-precision measurements, we keep the sputtering times of samples and standards equal.

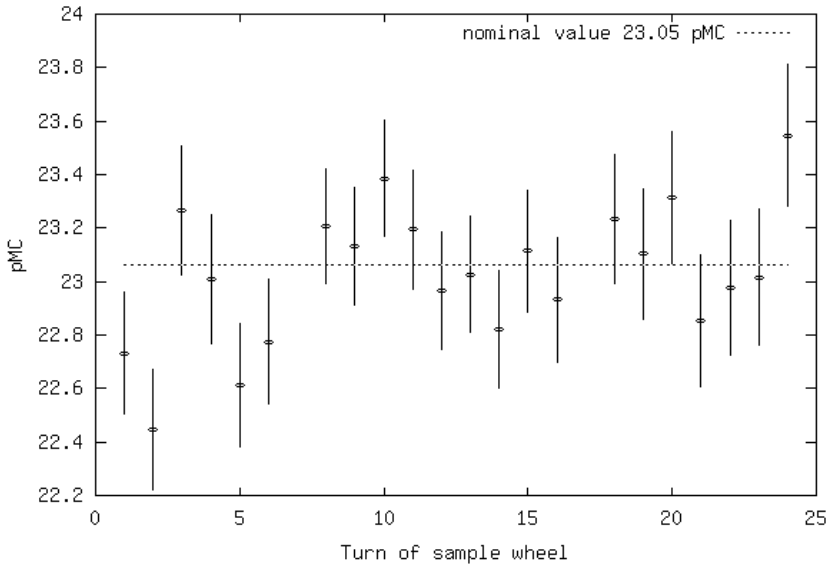


Figure 1 Cratering of sputter targets. In every turn of the sample wheel, an IAEA C-5 wood standard (23.05 pMC) was measured about twice as long as IAEA C-6 sucrose (150.61 pMC). The total sputtering time was 4.9 hr for the C-5 and 2.2 hr for C-6, respectively. The real time (including 38 other samples) was 3 days. The machine was retuned after turns 6 and 16 to eliminate the influence of machine drifts. Shown is the development of the measured pMC value of C-5 evaluated as an unknown sample, with the C-6 used as standard. The slight trend visible is most likely an artifact of retuning.

The fact that ion optical beam losses reduce measurement precision has been demonstrated by Rom et al. (1998). The main limiting aperture in VERA is the stripper canal (8 and 9 mm diameter at the entrance and exit, respectively). Figure 2 shows the progress we have achieved in accelerator transmission since the installation of VERA. It should be noted that the transmission shown is defined as $^{12}\text{C}^{3+}/^{12}\text{C}^-$ and includes the stripping yield to the 3+ charge state. Therefore, the values obtained with different stripper gases are shown with different symbols. From 1996 to 2002, argon was used as the stripper gas. In 2002, we switched to oxygen because this increased the stripping yield for 5+ charge states of very heavy ions by a factor of ~ 2 , whereas it lowered the $^{12}\text{C}^{3+}$ only by a factor of ~ 0.95 . The transmission for a randomly selected subset of all ^{14}C sputter targets measured so far at VERA is shown in Figure 2. Each data point corresponds to one sputter target, and one vertical set of data points corresponds to targets from the same sample wheel. The main reason for the present reliably high transmission is the use of the AUTOMAX program (Steier et al. 2000) for routine tuning. A previously limiting aperture of a small Wien filter in our analyzer (see Kutschera et al. 1997) was removed when the Wien filter was replaced by a large new electrostatic analyzer in January 2001 (Vockenhuber et al. 2003). Although ^{14}C measurements were not the primary motivation for this change, they have improved, since tuning of the analyzer is now less critical.

Although machine tuning adheres strictly to a fixed procedure, occasionally a “bad” beam tuning compromises the reproducibility of the measured isotopic ratios. This can be seen in Figure 1, where tuning took place before turn 1 and after turns 6 and 16 of the sample wheel. The scatter for the first tuning is obviously larger.

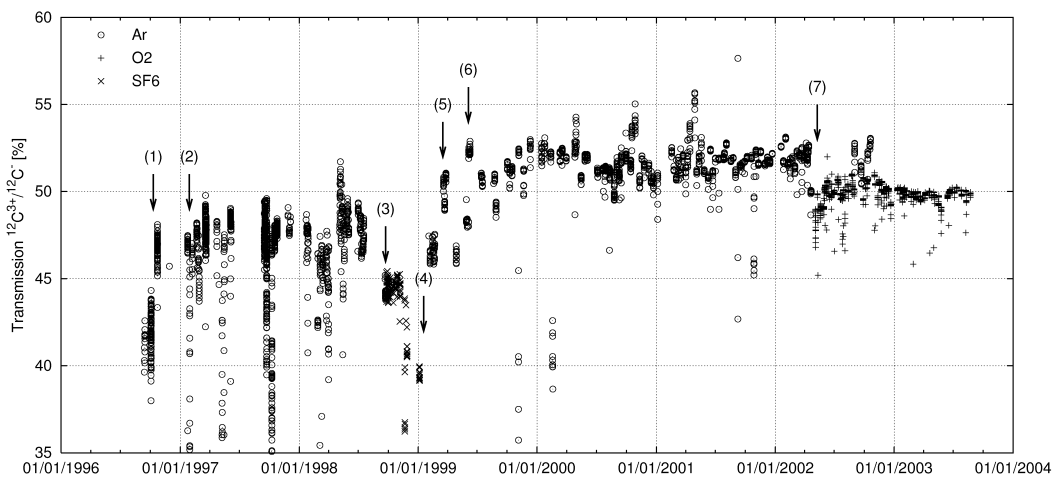


Figure 2 Progress in accelerator transmission. For the definition of the transmission, see the text. The following changes had significant influence: (1) Installation of the correcting quadrupole for the flawed injector magnet (see Priller 2000); (2) “manual” tuning procedure established; (3) sudden decrease in transmission for initially unknown reason; (4) reason found: SF_6 leak into stripper tube; (5) ion optical investigations of injector improve manual tuning procedure; (6) first use of a complete injector setup found by automatic tuning program AUTOMAX (Steier et al. 2000); (7) change from argon to oxygen as stripper gas.

Since we use a new spherical ionizer supplied by the Australian National University (ANU) (Weisser et al. 2002), we observe $^{12}\text{C}^-$ beams up to $\sim 80 \mu\text{A}$. However, in ^{14}C measurements with such currents, we encountered a significant dependency of the accelerator transmission on the beam current and a reduced measurement precision (see Figure 3). We interpret this current dependency as a space charge effect. The transmission profile became flat again when we changed our procedures to using a strong $^{12}\text{C}^-$ beam to tune the injector, instead of the previously used $^{13}\text{C}^-$ beam. Although this procedure restored the precision for routine dating, we try to stay between 40 and 50 μA for high-precision measurements.

Machine drifts can affect the precision since the standard and the sample are not measured at the same time. We perform runs of about 5-min duration on a sputter target before switching to the next one, so each of the 40 sputter targets is measured once every 3 hr. Only machine drifts which are faster will influence precision. In many measurements, we observe slow, parallel variations in the $^{13}\text{C}^{3+}/^{12}\text{C}^{3+}$ ratio of both the standard and the sample. Similar effects for the $^{14}\text{C}^{3+}/^{12}\text{C}^{3+}$ ratio are obscured by too-low counting statistics in the individual runs.

A severe problem arises if the tuned machine setup is subsequently worsened by long-term machine drifts to an extent that the ion optical transmission is compromised. In order to reach the required counting statistics for high-precision measurements, we have to run for several days. In this case, we retune the machine once every 24 hr.

$^{16}\text{O}:^{17}\text{O}:^{18}\text{O}$ as a Proxy for $^{12}\text{C}:^{13}\text{C}:^{14}\text{C}$

The use of oxygen isotopes instead of carbon isotopes to study machine fractionation has 3 main advantages. First, ^{16}O , ^{17}O , and ^{18}O are all stable isotopes, providing measurable beam currents. Thus, almost instantaneously a precision is reached which would require hours of ^{14}C event counting. Second, the ^{17}O beam can be measured and investigated at any point along the beam line with beam profile monitors and Faraday cups, whereas ^{14}C can only be detected in the final particle

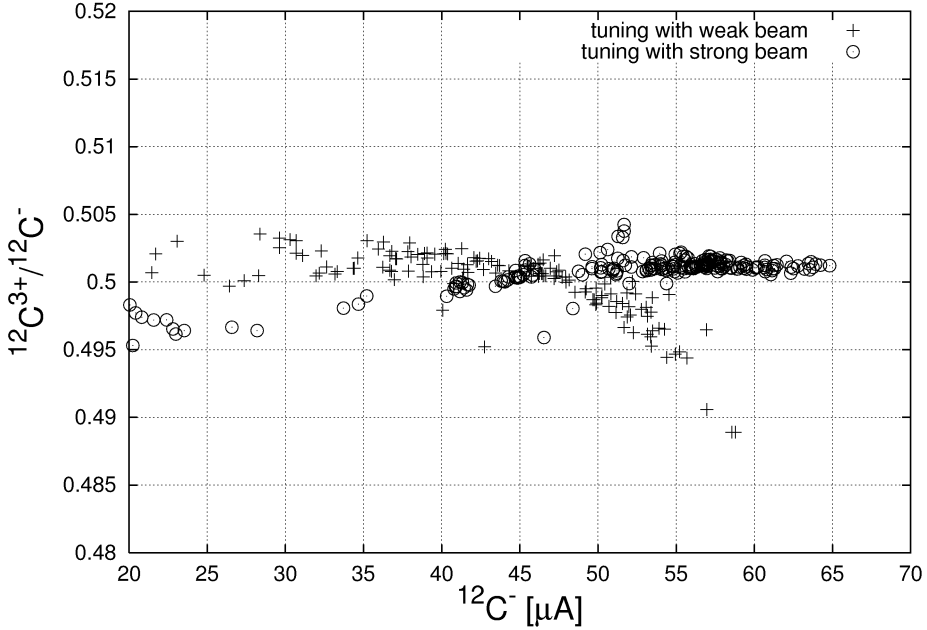


Figure 3 Accelerator transmission versus $^{12}\text{C}^-$ current for 2 different beam tunings. The transmission is measured as $^{12}\text{C}^{3+}/^{12}\text{C}^-$ and includes the stripping yield. If we tune the injector for a weak beam ($\sim 0.5 \mu\text{A } ^{13}\text{C}^-$), the transmission falls off for high beam currents (crosses). We attribute this to a space charge effect. This can be compensated by using a strong beam ($\sim 50 \mu\text{A } ^{12}\text{C}^-$) for tuning (circles). Interestingly, the setup obtained for the strong beam is also valid for sputter targets with low current yield, despite the apparent slight drop in transmission for low currents. This is caused by targets at the end of their lifetime.

detector. This helps to assess the origin of deviations in the isotopic ratios. And third, the $^{18}\text{O}/^{16}\text{O}$ ratio of all terrestrial material is $\sim 2 \times 10^{-3}$ within a few percent, whereas the $^{14}\text{C}/^{12}\text{C}$ can lie anywhere between 0 and $\sim 2 \times 10^{-12}$. For the value

$$F_{16,17,18} = (^{18}\text{O}^{3+}/^{16}\text{O}^{3+}) \div (^{17}\text{O}^{3+}/^{16}\text{O}^{3+})^2 \quad (4),$$

which is corrected for strictly mass-dependent fractionation, the variability is even smaller (Thiemens 1999). Therefore, in contrast to carbon, a small oxygen contamination will not alter the isotopic signature of the sample. Thus, oxygen allows us to study machine fractionation separately from contamination.

In a first test of this idea, we used 9 targets of commercial Al_2O_3 mixed with copper powder which were distributed evenly around the target wheel and measured with our usual ^{14}C measurement procedure, but with much shorter run times. Since VERA is a universal AMS facility, this can be easily achieved by slightly modifying magnetic fields and adjusting the offset-cup positions. With respect to the machine, the oxygen isotopes should behave very similar to carbon. The low isotopic abundance of ^{17}O (currents below 10 nA) was not a problem either for the tuning or for the measurement. Seven runs were performed on each target. It should be noted that these first experiments were too short to be sensitive to long-term machine drifts.

The observed reproducibility of the value $F_{16,17,18}$ (Equation 4) is 0.4%. This is significantly better than the reproducibility of the raw $^{17}\text{O}^{3+}/^{16}\text{O}^{3+}$ and $^{18}\text{O}^{3+}/^{16}\text{O}^{3+}$ (see Figure 4). If the same precision is achieved for carbon, it corresponds to ± 4 ^{14}C yr. This suggests that the AMS measurement is more

precise regarding the pMC value than for $\delta^{13}\text{C}$, provided there are sufficient counting statistics. This measurement also demonstrates that our Faraday cup electronics does not impose a precision limit.

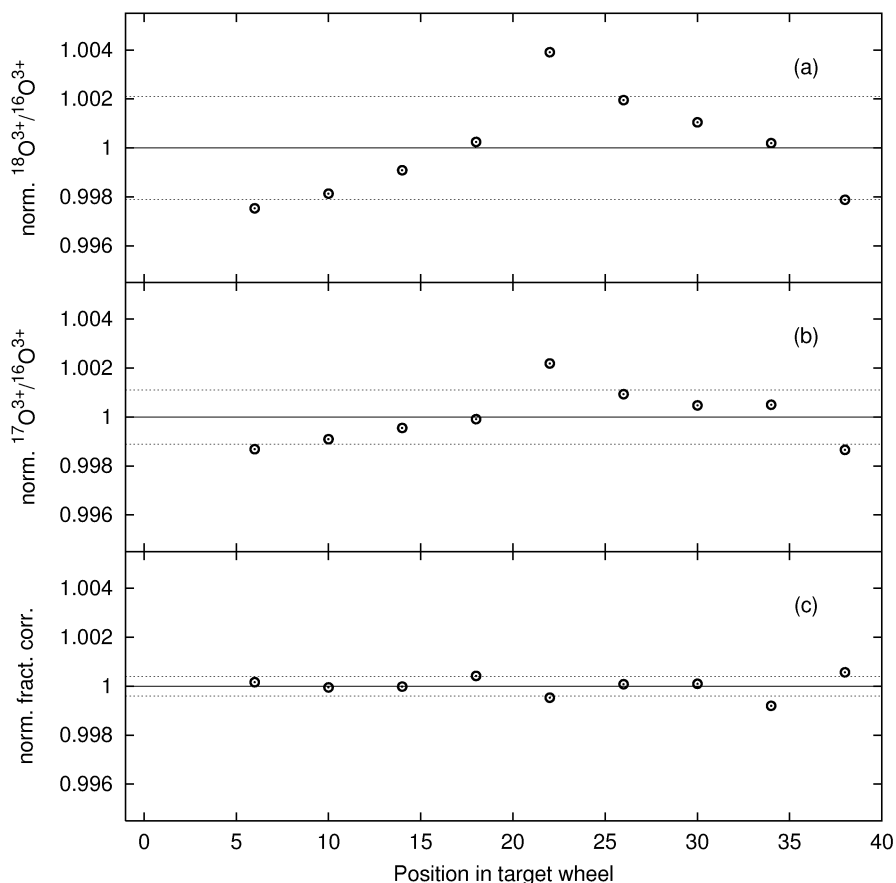


Figure 4 Measurement precision for fractionation-corrected isotopic ratios of oxygen. In the raw $^{17}\text{O}^{3+}/^{16}\text{O}^{3+}$ (a) and $^{18}\text{O}^{3+}/^{16}\text{O}^{3+}$ (b) data, systematic deviations between the targets are clearly visible, showing mainly a sinusoidal trend with their position in the wheel (eccentricity, see text). The standard deviation (indicated by the dithered lines) is 2.1‰ for $^{18}\text{O}^{3+}/^{16}\text{O}^{3+}$ and 1.1‰ for $^{17}\text{O}^{3+}/^{16}\text{O}^{3+}$. After applying the quadratic fractionation correction, the standard deviation is reduced to 0.4‰ (c).

“Turnwise” Evaluation

All new findings described above were taken into account by modifications of our automatic evaluation software “EVALGEN” (Puchegger et al. 2000). Previously (Rom et al. 1998), we first averaged the measured $^{13}\text{C}^{3+}/^{12}\text{C}^{3+}$ and $^{14}\text{C}^{3+}/^{12}\text{C}^{3+}$ ratios, and then applied blank and fractionation correction and standard normalization (Equations 1, 2, and 3). In the new scheme, the data of every turn of the sample wheel (one ~5-min run on every sputter target) is evaluated independently, and then the pMC values are averaged.

External uncertainties, which previously were calculated from the reproducibility of the raw $^{13}\text{C}^{3+}/^{12}\text{C}^{3+}$ and the $^{14}\text{C}^{3+}/^{12}\text{C}^{3+}$, are now determined from the pMC values. This new calculation scheme applies for the estimation of the scatter between the various ~5-min runs on 1 target (*inter-run scatter*, S_{IR}), the scatter between the sputter targets of the same graphite (*inter-target scatter*, S_{IT}),

and the scatter between independently prepared “graphites” from the same sample material (*inter-chemistry scatter*, S_{IC}). The S_{IC} is estimated from the scatter of the normalization factors $pMC_{\text{standard,nominal}}/F_{12,13,14,\text{standard}}$ in Equation 3 for different standards.

In the old evaluation scheme, the uncertainty was overestimated, as revealed by the investigations above. The modified scheme allows a significant reduction of the quoted error, shortening the measurement time for routine measurements.

True Wood Samples

In a final systematic investigation, we determined the maximum measurement precision possible at VERA for natural samples with a reasonable increase of effort. As material for the investigations, we chose the dendrochronologically-dated Scottish pine wood (3200–3239 BC), that is sample D of the Fourth International Radiocarbon Intercomparison (Scott et al. 2003).

From a total of 40 tree rings, we used 10 tree rings from the oldest section (3239–3230 BC) and 10 tree rings from the youngest section (3209–3200 BC). Each decade was sampled evenly by carving and homogenizing with a scalpel. Aliquots underwent separate chemical pretreatment. Additionally, standard samples from IAEA C-3 cellulose, IAEA C-5 wood, and IAEA C-6 sucrose were prepared. Samples, standards (except the sucrose), and a graphite ^{14}C blank had to undergo our standard procedure of acid-base-acid (ABA) chemical pretreatment with 1 mol/L HCl and 0.1 mol/L NaOH. Two sub-aliquots (10 mg) of each material were then oxidized separately in flame-sealed quartz tubes with 1 g CuO each, and Ag-wire to bind halogens and sulfur. The CO_2 was reduced with H_2 and Fe as catalyst at 610 °C according to the method of Vogel et al. (1984).

Since the sample material was divided in every step, a tree-like structure emerged (see Table 2). If a deviation from the nominal values is observed in the measured values, this scheme allows us to determine in which step the problem occurred.

Whereas a routine ^{14}C measurement for 1 sample wheel (40 sputter targets) reaches the required precision of <40 ^{14}C yr after about 24 hr, the duration of this systematic measurement was extended to 3 days. The machine was retuned on different sputter targets once per day. The average $^{12}\text{C}^-$ current was kept between 40 and 50 μA to avoid space charge effects, and all samples were measured equally long. Exhausted samples were skipped from further measurements once their current output dropped below ~ 25 μA .

The typical 1- σ uncertainty achieved for single targets is ± 20 ^{14}C yr (Figure 5). Our combined result for the 20 sputter targets from the earlier decade is 4493 ± 12 BP and 4524 ± 13 BP for the 8 targets of the later decade. This agrees well with the values taken from the INTCAL98 (Stuiver et al. 1998), 4492.1 ± 7.7 BP and 4531.7 ± 9.5 BP. Seven of the 28 targets deviate from the INTCAL98 value by more than 1 σ , which is compatible with the statistics. Four of these targets originate from the same ABA treatment (FD/F in Table 2). The combined ^{14}C age result of these targets is 33 ± 15 yr too high, indicating a contamination in the ABA step. No single target deviates by more than 2 σ .

The validity of this precision was demonstrated recently also by measurements on dendrochronologically dated wood of a new Stone Pine Chronology (Dellinger et al., these proceedings). For 58 tree-ring samples of this project, a total uncertainty of ~ 20 yr was achieved by single graphitizations, with each graphite split into 2 sputter targets. Thirty-three data points out of 58 agree within 1 σ with the INTCAL98 calibration curve, while only 2 points deviate by more than 2 σ .

On the other hand, the standard materials prepared for the Stone Pine measurement support the notion that the ABA step is a stage of possible contamination. For that measurement, 12 batches of

Table 2. ^{14}C ages for true wood samples. Ten tree rings from the earliest section and 10 tree rings from the latest section of the FIRI-D wood (Scott 2003) were prepared. Five aliquots of the older decade and 2 aliquots of the younger decade underwent separate chemical pretreatment. In each step of the measurement, the samples were divided, leading to a tree-like structure. The results of the individual sputter targets and also the combined results for each step are shown. For the FIRI-D samples, (d) is the measured result of each individual sputter target, (c) shows the combined results for both targets from the same graphitization, (b) the combined results for all 4 targets from the same ABA treatment, and (a) the combined result for all targets of the earlier and the later decadal section, respectively.

Sampling and homogenization with scalpel		ABA treatment		Graphitization		Sputter target			
Section	INTCAL98 ^{14}C age (BP)	Combined VERA ^{14}C age (a) (BP)	Label	Combined VERA ^{14}C age (b) (BP)	Label	Combined VERA ^{14}C age (c) (BP)	Label	Combined VERA ^{14}C age (d) (BP)	
Later decade 3209–3200 BC	4531.7 \pm 9.5	4524 \pm 13	FD/1	4525 \pm 14	FD/11	4518 \pm 17	FD/11a	4522 \pm 20	
			FD/2	4523 \pm 14	FD/21	4533 \pm 15	FD/11b	4514 \pm 19	
	4492.1 \pm 7.7	4493 \pm 12	4475 \pm 14	FD/A	4475 \pm 14	FD/A1	4580 \pm 19	FD/21a	4528 \pm 18
				FD/B	4490 \pm 13	FD/A2	4471 \pm 15	FD/21b	4498 \pm 24
			FD/C	4489 \pm 13	FD/B1	4499 \pm 15	FD/22a	4528 \pm 17	
			FD/D	4490 \pm 13	FD/B2	4479 \pm 15	FD/22b	4523 \pm 23	
			FD/E	4490 \pm 13	FD/C1	4487 \pm 14	FD/A1a	4466 \pm 20	
			FD/F	4525 \pm 13	FD/C2	4494 \pm 14	FD/A1b	4492 \pm 19	
			FD/G	4490 \pm 13	FD/E1	4491 \pm 15	FD/A2a	4477 \pm 18	
			FD/H	4490 \pm 13	FD/E2	4489 \pm 15	FD/A2b	4463 \pm 21	
Earlier decade 3239–3230 BC	4492.1 \pm 7.7	4493 \pm 12	FD/I	4490 \pm 13	FD/B1a	4486 \pm 24	FD/B1a	4486 \pm 24	
			FD/J	4490 \pm 13	FD/B2a	4479 \pm 15	FD/B1b	4507 \pm 17	
	4492.1 \pm 7.7	4493 \pm 12	4489 \pm 13	FD/K	4489 \pm 13	FD/C1a	4484 \pm 17	FD/B2a	4480 \pm 17
				FD/L	4490 \pm 13	FD/C1b	4491 \pm 17	FD/B2b	4476 \pm 23
			FD/M	4490 \pm 13	FD/C2a	4494 \pm 17	FD/C1a	4484 \pm 17	
			FD/N	4490 \pm 13	FD/C2b	4490 \pm 17	FD/C1b	4491 \pm 17	
			FD/O	4490 \pm 13	FD/E1a	4491 \pm 15	FD/C2a	4494 \pm 17	
			FD/P	4490 \pm 13	FD/E1b	4484 \pm 17	FD/C2b	4490 \pm 17	
			FD/Q	4490 \pm 13	FD/E2a	4482 \pm 19	FD/E1a	4497 \pm 19	
			FD/R	4490 \pm 13	FD/E2b	4493 \pm 19	FD/E1b	4484 \pm 17	
FD/S	4490 \pm 13	FD/F1a	4525 \pm 17	FD/E2a	4482 \pm 19				
FD/T	4490 \pm 13	FD/F1b	4514 \pm 20	FD/F1a	4525 \pm 17				
FD/U	4490 \pm 13	FD/F2a	4535 \pm 23	FD/F1b	4514 \pm 20				
FD/V	4490 \pm 13	FD/F2b	4526 \pm 18	FD/F2a	4535 \pm 23				
FD/W	4490 \pm 13	FD/F2b	4526 \pm 18	FD/F2b	4526 \pm 18				

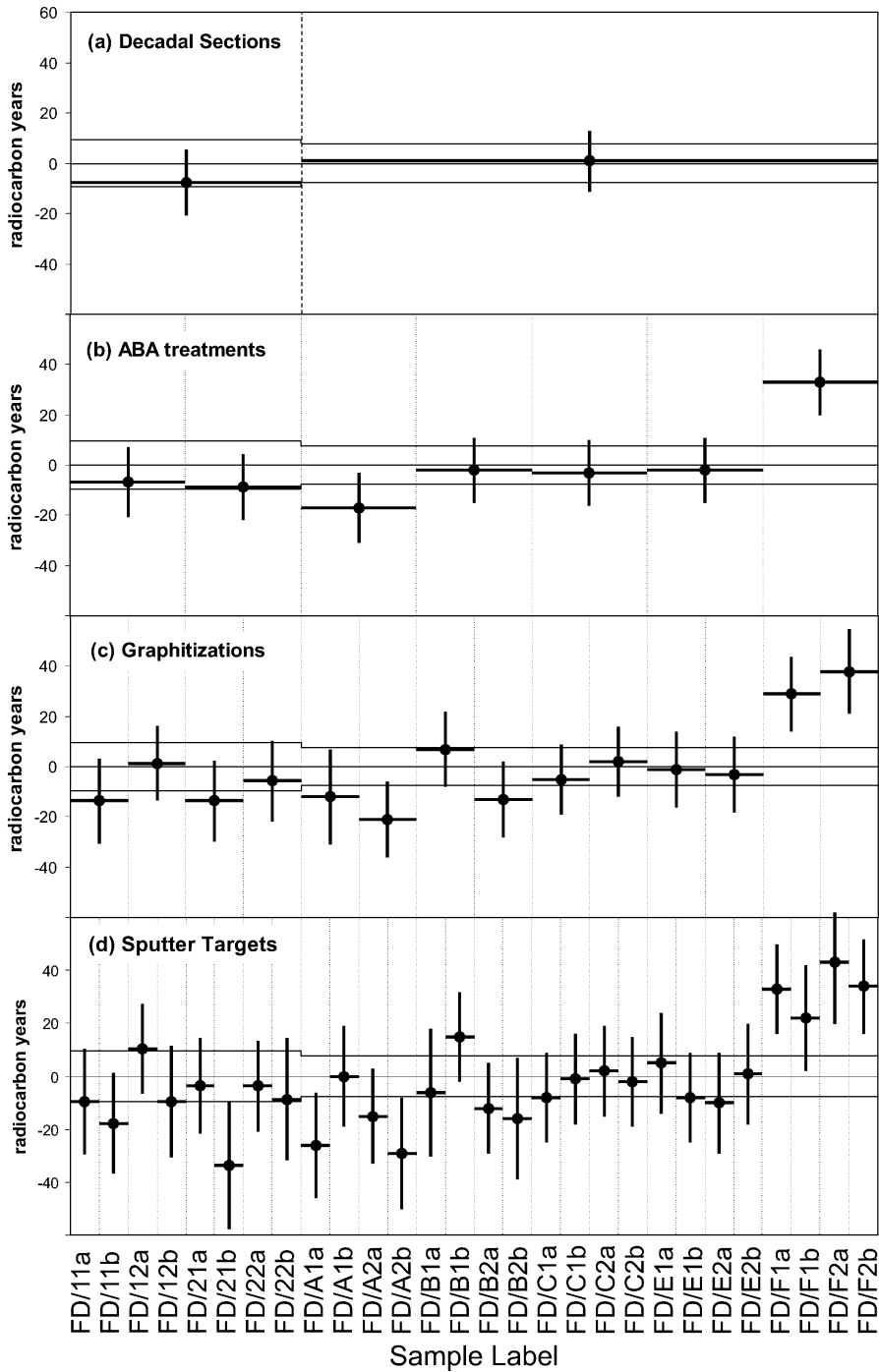


Figure 5 Deviation of FIRI-D sub-samples from the INTCAL98 master values. The values measured at VERA are shown for each individual sputter target in (d), (a), (b), and (c) are combined results. The labelling agrees with Table 2. The lines indicate the value of INTCAL98 and its uncertainty (all uncertainties are 1σ).

standard material underwent separate ABA treatment. Afterwards, the material was split into several sputter targets. For one of the 12 ABA treatments of standard material, all 4 targets were consistently measured ~ 55 ^{14}C yr too old. However, all observed deviations are too small to be significant at the precision level of routine measurements.

SUMMARY AND OUTLOOK

By systematically exploring the uncertainties in our AMS measurement and sample preparation procedures, we were able to increase our measurement precision significantly.

Systematic measurements suggest that for the AMS machine, the precision of the fractionation corrected values is better than 1%. We think that the use of oxygen as an isotopic template for carbon measurements, which was explored in this work, will be a significant advantage in further systematic measurements.

For the chemical sample preparation, a general quantification of their contribution to uncertainty cannot be given, since real samples vary significantly in their chemical composition, and the level of contamination is different. However, we recently achieved an overall precision of ± 20 ^{14}C yr (1σ) for 50 dendrochronologically-dated wood samples in the period from 3500 to 3000 BC (Dellinger et al., these proceedings). This was achieved without preparing replicates and by counting $^{14}\text{C}^{3+}$ ions for 3 to 4 hr on every sample. There is an indication that laboratory contamination during the chemical sample preparation contributes to the final uncertainty also for samples of good quality.

Investigations by Niklaus et al. (1994) on the wiggles of the tree-ring calibration curve show that an improved precision of ± 20 ^{14}C yr will also translate into smaller uncertainty intervals for the calibrated ages. However, whether this increased ^{14}C dating precision is true has to be investigated carefully. Probably systematic deviations will become significant which are caused by different sample material and quality. Additional deviations may be caused by regional offsets (Goodsite et al. 2001), seasonal variations (Dellinger et al., these proceedings; Kromer et al. 2001), or non-quadratic fractionation in nature (Wigley and Muller 1981). Up to now, such possible deviations often evaded investigation, since high measurement precision is a prerequisite for their study. Therefore, investigations on the accuracy of the ^{14}C dating method itself will most likely be the first application of increased measurement precision.

REFERENCES

- Dellinger F, Nicolussi K, Kutschera W, Schiebling P, Steier P, Wild EM. 2004. A ^{14}C calibration with AMS from 3500 to 3000 BC, derived from a new high-elevation stone-pine tree ring chronology. *Radiocarbon*, these proceedings.
- Ferry JA. 1993. Recent developments in electrostatic accelerator technology at NEC. *Nuclear Instruments and Methods in Physics Research A* 328:28–33.
- Finkel RC, Suter M. 1993. AMS in the earth sciences: technique and applications. *Advances in Analytical Geochemistry* 1:1–114.
- Goodsite ME, Rom W, Heinemeier J, Lange T, Ooi S, Appleby PG, Shotyk W, van der Knaap WO, Lohse C, Hansen TS. 2001. High-resolution AMS ^{14}C dating of post-bomb peat archives of atmospheric pollutants. *Radiocarbon* 43(2B):495–515.
- Kromer B, Manning SW, Kuniholm PI, Newton MW, Spurk M, Levin I. 2001. Regional $^{14}\text{CO}_2$ offsets in the troposphere: magnitude, mechanism, and consequences. *Science* 294:2529–32.
- Kutschera W, Collon P, Friedmann H, Golser R, Hille P, Priller A, Rom W, Steier P, Tagesen S, Wallner A, Wild E, Winkler G. 1997. VERA: a new AMS facility in Vienna. *Nuclear Instruments and Methods in Physics Research B* 123:47–50.
- Nadeau M-J, Kieser WE, Beukens RP, Litherland AE. 1987. Quantum mechanical effects on sputter source isotope fractionation. *Nuclear Instruments and Methods in Physics Research B* 29:83–6.
- Niklaus TR, Bonani G, Suter M, Wölfli W. 1994. Systematic investigation of uncertainties in radiocarbon dating due to fluctuations in the calibration curve. *Nuclear Instruments and Methods in Physics Research B* 92:194–200.

- Priller A, Golser R, Hille P, Kutschera W, Rom W, Steier P, Wallner A, Wild E. 1997. First performance tests of VERA. *Nuclear Instruments and Methods in Physics Research B* 123:193–8.
- Priller A, Brandl T, Golser R, Kutschera W, Puchegger S, Rom W, Steier P, Vockenhuber C, Wallner A, Wild E. 2000. Extension of the measuring capabilities at VERA. *Nuclear Instruments and Methods in Physics Research B* 172:100–6.
- Puchegger S, Rom W, Steier P. 2000. Automated evaluation of ^{14}C AMS measurements. *Nuclear Instruments and Methods in Physics Research B* 172:274–80.
- Rom W, Golser R, Kutschera W, Priller A, Steier P, Wild E. 1998. Systematic investigations of ^{14}C measurements at the Vienna Environmental Research Accelerator. *Radiocarbon* 40(1):255–63.
- Scott EM. 2003. Section I: The Fourth International Radiocarbon Intercomparison (FIRI). *Radiocarbon* 45(2):135–50.
- Steier P, Puchegger S, Golser R, Kutschera W, Priller A, Rom W, Wallner A, Wild E. 2000. Developments towards a fully automated AMS system. *Nuclear Instruments and Methods in Physics Research B* 161–163: 250–4.
- Stuiver M, Polach HA. 1977. Discussion: reporting of ^{14}C data. *Radiocarbon* 19(3):355–63.
- Stuiver M, Reimer PJ, Bard E, Beck JW, Burr GS, Hughen KA, Kromer B, McCormac G, van der Plicht J, Spurk M. 1998. INTCAL98 radiocarbon age calibration, 24,000–0 cal BP. *Radiocarbon* 40(3):1041–83.
- Thiemens MH. 1999. Mass-independent isotope effects in planetary atmospheres and the early solar system. *Science* 283:341–5.
- Vockenhuber Ch, Ahmad I, Golser R, Kutschera W, Liechtenstein V, Priller A, Steier P, Winkler S. 2003. Accelerator mass spectrometry of heavy long-lived radionuclides. *International Journal of Mass Spectrometry* 223–224:713–32.
- Vogel JS, Southon JR, Nelson DE, Brown T. 1984. Performance of catalytically condensed carbon for use in accelerator mass spectrometry. *Nuclear Instruments and Methods in Physics Research B* 5:289–93.
- Weisser DC, Lobanov NR, Hausladen PA, Fifield LK, Wallace HJ, Tims SG, Apushinsky EG. 2002. Novel matching lens and spherical ionizer for a cesium sputter ion source. *PRAMANA - Journal of Physics, Indian Academy of Sciences* 59:997–1006.
- Wigley TML, Muller AB. 1981. Fractionation corrections in radiocarbon dating. *Radiocarbon* 23(2):173–90.
- Wild E, Golser R, Hille P, Kutschera W, Priller A, Puchegger S, Rom W, Steier P, Vycudilik W. 1998. First ^{14}C results from archaeological and forensic studies at the Vienna Environmental Research Accelerator. *Radiocarbon* 40(1):273–81.